SAND2014-19729J

EPJ manuscript No.
(will be inserted by the editor)

Dynamic High-Temperature Tensile Characterization of an Iridium Alloy with Kolsky Tension Bar Techniques

Bo Song[1,a], Kevin Nelson[2], Ronald Lipinski[1], John Bignell[1], G. B. Ulrich[3], and E. P. George[3]

[1] Sandia National Laboratories, Albuquerque, NM 87185, USA
[2] Sandia National Laboratories, Livermore, CA 94550, USA
[3] Oak Ridge National Laboratory, Oak Ridge, TN 37831, USA

Abstract. Kolsky tension bar techniques were modified to characterize an iridium alloy in tension at elevated strain rates and temperatures. The specimen was heated to elevated temperatures with an induction coil heater before dynamic loading; whereas, a cooling system was applied to keep the bars at room temperature during heating. A preload system was developed to generate a small pretension load in the bar system during heating in order to compensate for the effect of thermal expansion generated in the high-temperature tensile specimen. A laser system was applied to directly measure the displacements at both ends of the tensile specimen in order to calculate the strain in the specimen. A pair of high-sensitivity semiconductor strain gages was used to measure the weak transmitted force due to the low flow stress in the thin specimen at elevated temperatures. The dynamic high-temperature tensile stress-strain curves of a DOP-26 iridium alloy were experimentally obtained at two different strain rates (∼1000 and 3000 s^{-1}) and temperatures (∼750 and 1030^oC). The effects of strain rate and temperature on the tensile stress-strain response of the iridium alloy were determined. The iridium alloy exhibited high ductilities in stress-strain response that depent strongly on strain-rate and temperature effects.

1 Introduction

Iridium alloys possess unique property combinations of high melting temperature, high-temperature strength and ductility, and excellent oxidation and corrosion resistance [1], making them ideal for high-temperature applications. In some high-temperature and high-speed impact applications, the high-temperature impact response of the material must be fully understood in order to meet the safety requirement for the design of components. High-strain-rate and high-temperature stress-strain data are thus needed to develop strain-rate and temperature dependent material models for safety analysis. However, current mechanical characterization of

[a] e-mail: bsong@sandia.gov

iridium alloys has been limited to relatively low strain rates (below 50 s^{-1}) [2] [3] [4] [5], which are not sufficiently high for their potential applications. Song et al. [6] [7] recently employed Kolsky compression bar testing, also known as split Hopkinson pressure bar testing, to characterize the compressive stress-strain properties of a DOP-26 iridium alloy at high strain rates (300 - 10000 s^{-1}) and high temperatures (750 and 1030^oC). The iridium alloy showed significant strain-rate and temperature effects on the compressive stress-strain response. However, the compression tests did not provide ductility and failure information at high strain rates and temperatures. Therefore, dynamic tensile characterization of iridium alloys at high temperatures was needed.

The Kolsky bar was originally developed for compression testing [8] and subsequently modified for use in tension and torsion testing [9] [10]. A variety of Kolsky tensile bar techniques have been developed since the 1960s [11]. The most commonly used method is direct-tension Kolsky bars [12] [13]. Recently, Song et al. [14] developed a direct-tension Kolsky bar that launches a solid striker to an end cap on the open end of the gun barrel to generate a dynamic tensile load in the bar system. In contrast to the compression tests, more attention must be paid to the Kolsky tensile tests due to the complications of specimen attachment to the bar ends. A dog-bone-shaped cylinder with threads on both ends is a typical specimen design for Kolsky tension bar tests. However, special fixtures are needed when characterizing thin sheet specimens. In addition, the complex specimen fixtures may modify the stress wave propagation. For instance, a stress wave reflection may be generated at each interface within the joints/fixtures between the specimen and the bars. In this case, the reflected wave, which is usually used to calculate the strain rate and strain in the specimen, is no longer reliable. Direct displacement measurements on both ends of the specimen are required.

It is very challenging to conduct high-temperature Kolsky tension bar experiments. For high-temperature Kolsky bar tests, which are typically in compression, it is common practice to heat the specimen individually while the whole bar system is kept at room temperature before dynamic loading. The high-temperature specimen is dynamically loaded immediately upon contact with the room-temperature bars. Cold contact time (CCT) has been defined as the time during which the high-temperature specimen stays in contact with the room-temperature bars until being dynamically loaded [11]. The CCT is usually required to be as short as several milliseconds, and even within one millisecond when the specimen is thin [7]. Appropriate modifications have been made to Kolsky compression bars for generating short CCTs. However, it has been difficult to directly apply these modifications to Kolsky tension bars. In a Kolsky tension bar test, the specimen has to be firmly attached to the bar ends before dynamic loading, which makes it nearly impossible to heat the specimen individually. Su et al. [15] applied thermal-protective coating with a very low heat transfer coefficient to the bar surface to mitigate the heat transfer to the bars. Using the same method, the temperature in the bars was reduced to below 300^oC when the specimen was heated to 527^oC by Guo and Gao [16]. This means the heat was still transferred from the high-temperature specimen to the bars through the threads, which generated a thermal gradient in the bars. Such a thermal gradient may become more significant when the testing temperature increases. A significant thermal gradient will result in erroneous stress and strain measurements in the specimen, particularly when the test temperature is over 600^oC where the Young's modulus of steel, a typical bar material, decreases significantly. These challenges limit current Kolsky tension bar tests to temperatures below 600^oC [15] [16] [17] [18] [19], where the effects of temperature gradients on the steel bars can be neglected [18]. However, special experimental design considerations are required for Kolsky tension bar experiments at higher temperatures, i.e., 750 and 1030^oC in this study.

In this study, the conventional Kolsky tension bar was modified to characterize dynamic tensile stress-strain response of a thin-sheet DOP-26 iridium alloy at elevated temperatures. The iridium alloy was characterized at two different strain rates ($\sim$1000 and 3000 s^{-1}) and temperatures ($\sim$750 and 1030^oC) in order to determine the effects of strain rate and temperature on the tensile stress-strain response.

2 Modified High-Temperature Kolsky Tension Bar System

In this study, the Kolsky tension bar described in [14] was modified for dynamic high-temperature characterization of the DOP-26 iridium alloy. Figure 1(a) shows a schematic of the modified high-temperature Kolsky tension bar system. Since it is not possible to directly thread a thin flat iridium specimen into the bar ends, a pair of specimen fixtures was designed, as shown in Fig. 1(b). The specimen was made into a flat dog-bone shape. The fixture was machined with a slot with the same dimensions as the non-gage section of the specimen such that the whole non-gage section of the specimen was placed into the slot of the fixture. The specimen was then covered with a semicircular cap. The depth of the fixture was made the same as the specimen thickness such that the semicircular cap did not provide additional perpendicular force on the specimen but retained the specimen during dynamic loading. Both the fixtures and the semicircular caps were made of Inconel 718 steel, which has relatively high strength at elevated temperatures.

An induction coil heater was installed on the testing section. Due to the small size of the specimen under investigation, the induction coil was set to heat the relatively large fixtures and then transfer the heat to the specimen (Fig. 1(c)). This experimental design enables direct measurement of displacements at the specimen ends using a laser. When the fixtures are heated with the induction coil, the heat is transferred to both the specimen and the bars simultaneously. In order to prevent heating of the bars, a pair of hollow water-cooled pillow blocks was installed on the bar ends, as shown in Fig. 1(d). This design is similar in principle to that developed by Scapin et al. [20]. The difference is that Scapin et al. [20] applied a Cortex-tube-based air cooling system to cool down the bars for testing up to 400^oC. The water cooling system used in this study was shown to be capable of cooling the bars below room temperature when the testing temperature was as high as 1030^oC.

As shown in Fig. 1(c), the high-temperature fixtures attached to the bar ends still generate a thermal gradient between the bars and the specimen even though the bars are kept at room temperature, which may modify the wave propagation. In addition, the complicated design of the fixtures themselves exhibits many interfaces that may modify the wave propagation. Both result in an unreliable reflected pulse for specimen strain calculation. As mentioned earlier, we employed a laser system to directly measure the displacement histories at the specimen ends of the fixtures. The working principle of the laser system is illustrated in Fig. 2. A uniform laser line generator was used as a light source and then split into two independent beams. The movements of the incident and transmission bars, which consequently stretches the specimen, generate the intensity changes of the laser beams that are independently detected with two seperate laser detectors. Therefore, the specimen strain can be calculated as

$$\epsilon = \frac{L_1 - L_2}{L_s} \tag{1}$$

where L_1 and L_2 are displacements of the specimen ends attached to the incident and transmission bars, respectively; L_s is the gage length of the specimen. As shown in Fig. 1(b), the non-gage sections of the specimen were enclosed in the fixtures. Equation (1)

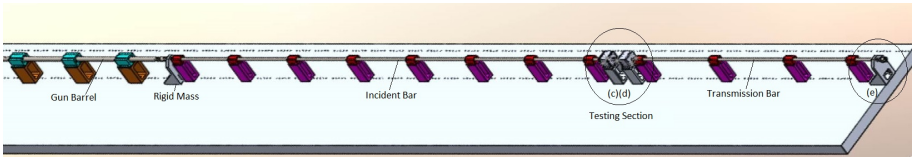

(a)

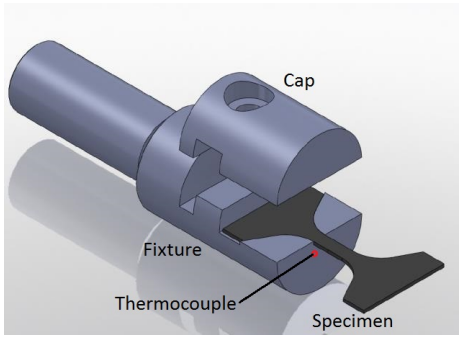

(b)

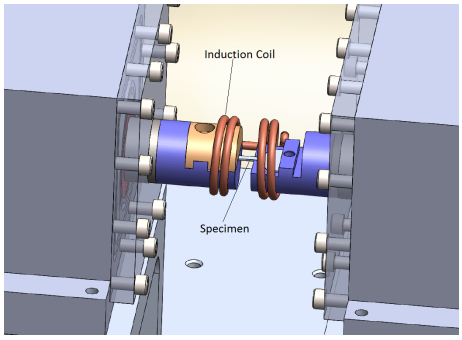

(c)

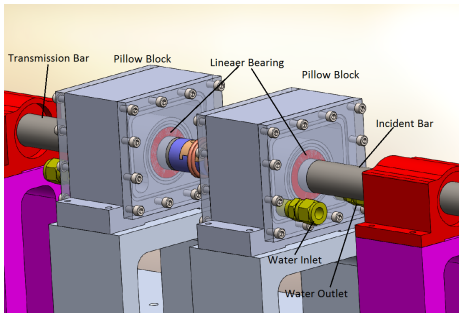

(d)

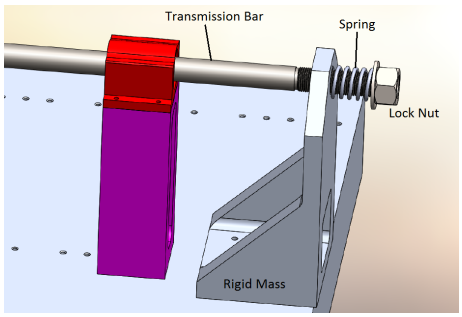

(e)

Fig. 1. High-temperature Kolsky tension bar setup

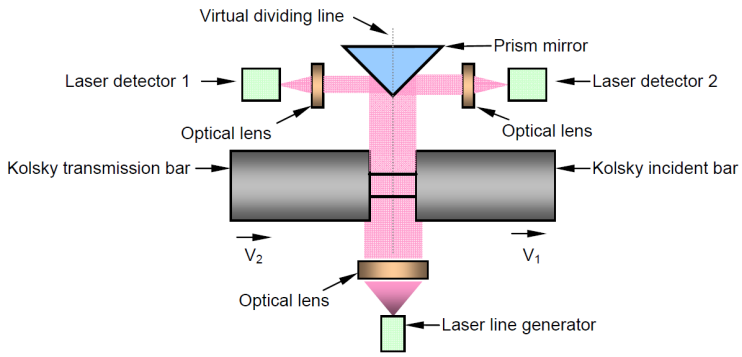

Fig. 2. The laser system for bar-end displacement measurement

maximizes the representation of the actual deformation of the gage section without the need for correction with respect to the deformation in the non-gage sections.

When the thin iridium specimen is heated, i.e. to 750 and 1030^oC in this study, the specimen may become longer due to thermal expansion. However, the force generated by such a thermal expansion may not be sufficiently high to overcome the friction between the bars and the bar supports and push the incident and transmission bars back. As a consequence, the thin iridium specimen may buckle. The buckling generated in the specimen will produce an erroneous stress-strain response which is difficult to correct. A spring-loaded pre-tension system, as shown in Fig. 1(e), was developed to prevent the specimen from buckling during heating. The spring was placed between a rigid mass and a flange screwed onto the free end of the transmission bar. Screwing the flange toward the rigid mass compresses the spring and in turn generates a tension load in the tension bar system. Another rigid mass was placed against the gun barrel (Fig. 1(a)) to prevent the bar system from moving backwards when the whole bar system is pre-loaded in tension[21]. In this study, the spring was set to generate a pre-tension load of approximately 18N which is sufficient to straighten the iridium specimen during heating but insufficient to produce further stretch on the iridium specimen.

Another high temperature testing issue is thermal softening of the specimen. In general, the flow stress in metallic materials decreases significantly at elevated temperatures, which results in a very weak transmitted signal in Kolsky bar experiments. In order to measure the weak transmitted signal with relatively high resolution, a pair of semiconductor strain gages was used to replace the regular resistor strain gages on the transmission bar. The semiconductor strain gages have a gage factor of 139, which is approximately 70 times more sensitive than the regular resistor strain gages. The specimen stress is calculated as

$$\sigma = \frac{E_0 A_0 \epsilon_t}{A_s} \tag{2}$$

where E_0 is Young's modulus of the bar material; A_0 is the cross-sectional area of the transmission bar; ϵ_t is the transmitted strain; and A_s is the cross-sectional area of the specimen. Combining the measurements of the semiconductor strain gages (Eq. (2)) and the laser system (Eq. (1)) for specimen stress and strain histories, respectively, yields the stress-strain curve of the specimen under investigation.

3 Dynamic High-Temperature Tensile Characterization of Iridium Alloy

In this study, the iridium tensile specimens were removed from prime DOP-26 alloy blanks using electrical discharge machining (EDM) with zinc-coated brass wire. The specimens were ground to remove the residual EDM layer, and then deburred and polished. All specimens were acid cleaned and then heat treated at $1075^oC \pm 25^oC$ for 1 hour$\pm$10 minutes in vacuum (1×10^{-4} torr). The tensile specimens had a thickness of 0.66 mm, a width of 2.54 mm, and a gage length of 6.35 mm. The detailed dimensions of the iridium specimens used in this study are shown in Fig. 3.

In order to check the temperature uniformity in the specimen during heating, three thermocouples were attached to the gage section of the iridium specimen: one was placed in the center and the other two were placed close to each end of the specimen, respectively, as shown in Fig. 4(a). Figure 4(b) shows the temperature histories from the three thermocouples when the induction heater was programmed to heat the specimen to 750^oC. The thermocouple signals were noisy with high frequencies caused

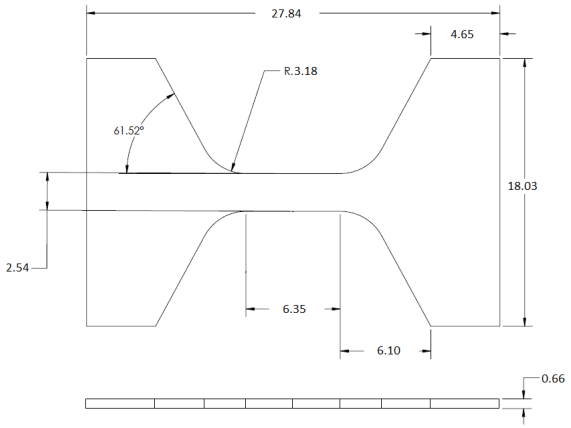

Fig. 3. Iridium tensile specimen (unit: mm)

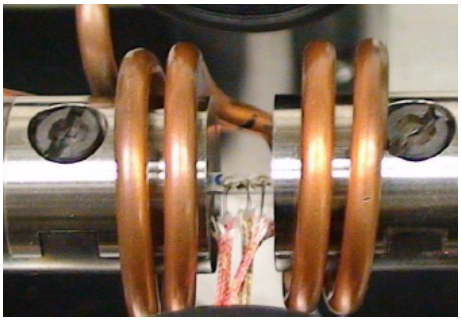

(*a*)

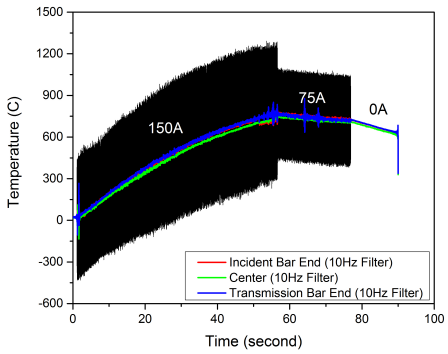

(*b*)

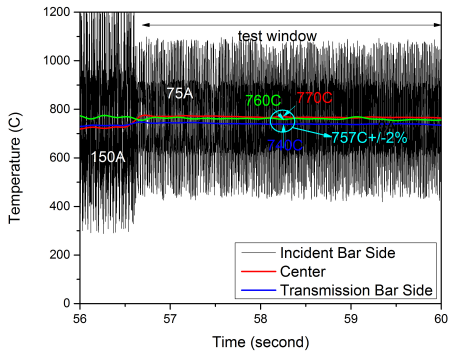

(*c*)

Fig. 4. Temperature uniformity during induction heating

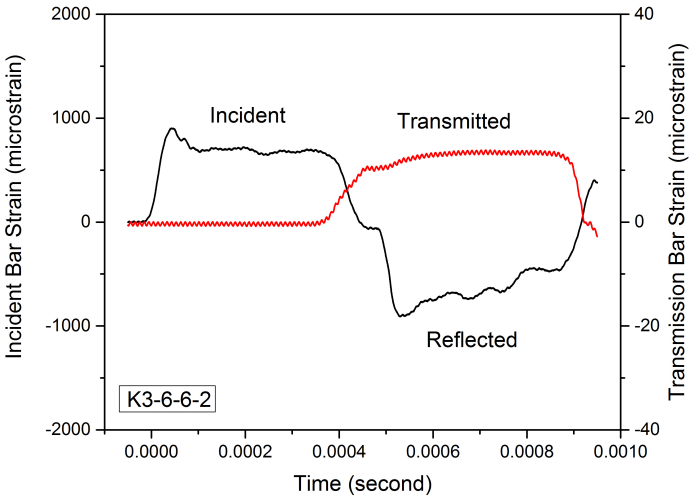

Fig. 5. Typical incident, reflected and transmitted signals

by the electromagnetic field generated by the induction coil. In order to provide clearer temperature readings, a 10Hz digital filter was applied to the thermocouple signals, the results of which are also shown in Fig. 4(b). It is noted that Fig. 4(b) records the whole heating process of the specimen. However, it takes much less time, usually 3-4 seconds (called "time window of testing" here), to complete the dynamic testing procedure, as marked in Figure 4(c). The temperatures were very consistent during the heating process as indicated by the thermocouples in three different locations. The results demonstrate the reasonable uniformity of the temperature across the whole specimen gage section ($756^oC \pm 2.3\%$). In actual iridium alloy testing, only one thermocouple was attached to the fixture surface under the specimen, as shown in Fig. 1(b), to avoid spot welding the thermocouple to the surface and causing specimen microstructure changes.

Figure 5 shows typical strain gage signals on the incident and transmission bars for the incident, reflected, and transmitted waves at the test temperature of 1030^oC. As shown in Fig. 5, the transmission bar strain was low (only 15 microstrains) due to the low strength of the iridium specimen at such a high temperature. High resolution measurement of the low transmitted signal was achieved by using high sensitivity semiconductor strain gages. Again, the reflected pulse is not reliable and cannot be used for specimen strain measurement. Instead, we used the laser system (Fig. 2) to directly track the movements of the specimen ends that were attached to the incident and transmission bars. The laser outputs are shown in Fig. 6. Figure 6 clearly shows significant change in the laser output for the front end (on the incident bar side) but no significant change for the back end (on the transmission bar side). This is because the transmitted force was too small to generate significant displacement on the transmission bar side.

The engineering stress and strain histories in the specimen, which were calculated with Equations (2) and (1), respectively, are shown in Fig. 7. The strain rate was then calculated with the slope of the strain history as a nearly constant 860 s^{-1}. It is noted that when the reflected pulse becomes unreliable, it is difficult to compare the force histories at both ends of the specimen for force/stress equilibrium checks.

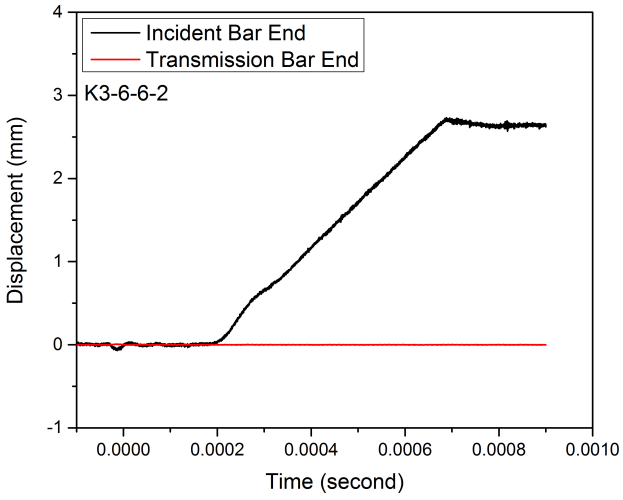

Fig. 6. Laser outputs for bar-end displacement measurements

In this study, we used high-rate high-temperature digital image correlation (DIC) approaches to qualitatively check the deformation uniformity across the whole specimen gage section. The DIC results showed that, under the same loading condition, the specimen with a gage length of 6.35 mm was deformed uniformly until necking occurred. However, due to the interaction between the high-intensity light for the DIC measurement and the laser system used for the direct strain measurement in the specimen, we were not able to apply DIC in each test. Based on the stress and strain histories shown in Fig. 7, the tensile stress-strain curves at 860 s^{-1} and 1030^oC were obtained as shown in Fig. 8. The stress-strain curves exhibit oscillations because of the effect of electromagnetic field generated by the induction coil on the highly-sensitive semiconductor strain gage signals. The raw stress-strain data was filtered to remove the oscillations, the result of which is also shown in Fig. 8.

Following the same procedure, the iridium alloy was characterized in tension at two different strain rates ($\sim$1000 and 3000 s^{-1}) and temperatures ($\sim$750 and 1030^oC). At each condition, three experiments were repeated and the results were consistent (within 10%) at the same testing condition. Figure 9 shows the mean tensile stress-strain curves of the iridium alloy at different strain rates and temperatures. It is noted that, due to the superior ductility of the iridium alloy at elevated temperatures, the specimens did not fail during the first dynamic tensile load except for the testing condition of 735^oC/3450 s^{-1}. At the condition of 735^oC/3450 s^{-1}, the specimens possessed engineering failure strains varying between 0.5 and 0.7. It is noted that the engineering failure strains were not representative of the tre failure strain since significant strain localization and necking occurred in the specimens before failure. Therefore, the stress-strain curves are plotted up to a strain of 0.5 in Fig. 9. The dynamic high-temperature stress-strain curves of the iridium alloy show different profiles than quasi-static curves [3]. All stress-strain curves show an initial elasticity followed by significant work hardening behavior when the strain is below 10%. This phenomenon may be related to a change in microstructure or deformation mechanism at high strain rates and elevated temperatures, which is still under investigation. Also, it is noted that, when the strain is below 10%, the stress-strain curves show

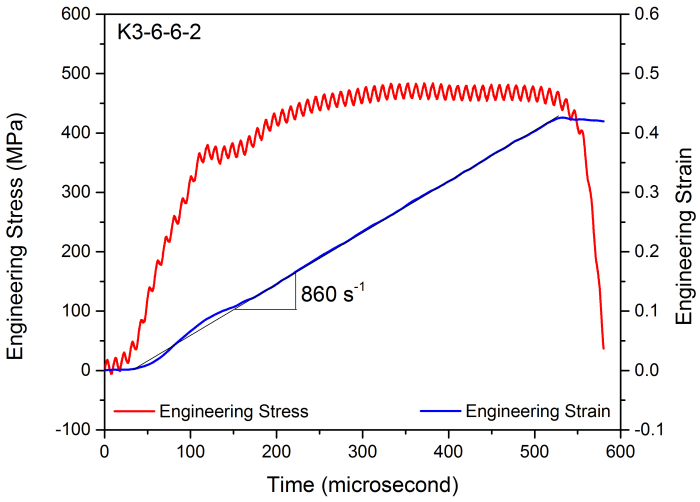

Fig. 7. Engineering stress and strain histories

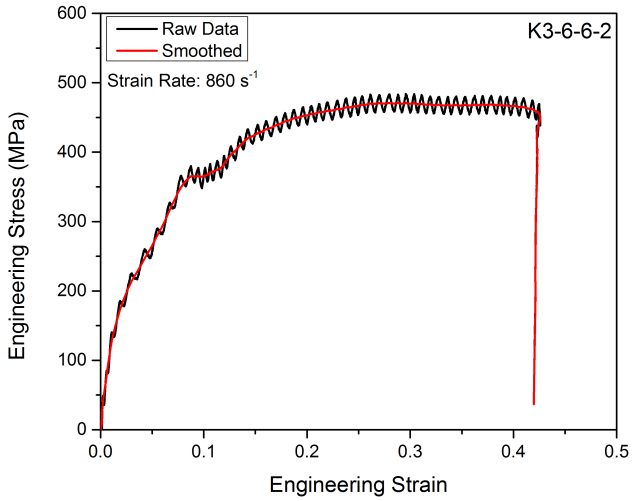

Fig. 8. Engineering tensile stress-strain curves at 860 s^{-1} and 1030^oC

neither strain-rate nor temperature effects. When the strain increases, the stress-strain curves show plastic flow with significant strain-rate and temperature effects. At strains greater than 10% and similar strain rates the flow stresses decrease when the temperature increases from 750 to 1030^oC, showing significant thermal-softening behavior. At the same temperature, the flow stresses increase when the strain rate increases from ∼1000 to 3500 s^{-1}, showing a positive strain-rate sensitivity. Detailed strain-rate effects on the tensile stress-strain response including the quasi-static data

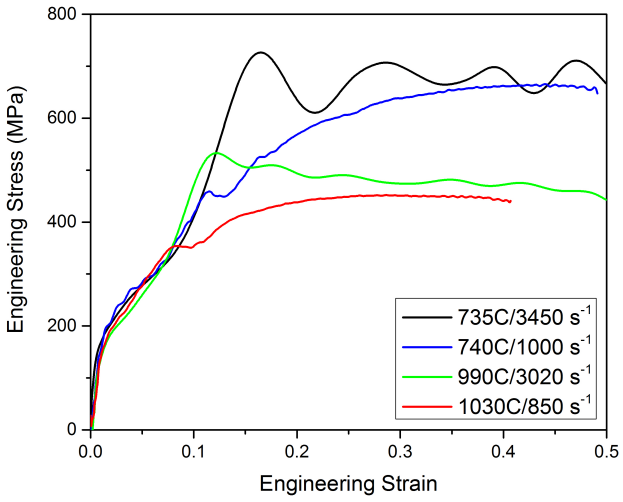

Fig. 9. Engineering stress-strain curves at different strain rates and temperatures

presented in [3] are shown in Fig. 10 at two different temperatures (750^oC (Fig. 10(a)) and $1030/1090^oC$ (Fig. 10(b)), respectively. The data obtained from this study were boxed and the rest are from the reference [3] in both figures. Figure 10 clearly shows a significant strain-rate effect on the tensile flow stress of the iridium alloy at both temperatures. The strain-rate sensitivities are slightly different at the two temperatures and are also dependent on the level of strain.

4 Summary

The conventional direct-tension Kolsky bar was modified for high-temperature tensile characterization of the DOP-26 iridium alloy. An induction coil was applied to heat the iridium specimen to elevated temperatures up to 1030^oC while the specimen ends of the incident and transmission bars were cooled to reduce the thermal gradient in the bars. A pair of semiconductor strain gages on the transmission bar was used to directly measure the force/stress in the specimen during dynamic loading. A laser system was developed to independently measure the displacements at the specimen ends on the incident- and transmission-bar sides so that the specimen strain could be calculated. A spring-loaded pretension system was installed on the free end of the transmission bar to prevent the high-temperature specimen from buckling during heating. Dynamic tensile stress-strain curves of the iridium alloy were obtained at two elevated temperatures (750 and 1030^oC) and strain rates ($\sim$1000 and 3000 s^{-1}). The iridium alloy shows high ductility at elevated temperatures and strain rates. The effects of strain rate and temperature on the tensile stress-strain response of the iridium alloy were also determined. The iridium alloy exhibits little sensitivity to strain rate or temperature when the strain is below 10% but strong sensitivities to both strain rate and temperature when the strain is greater than 10%.

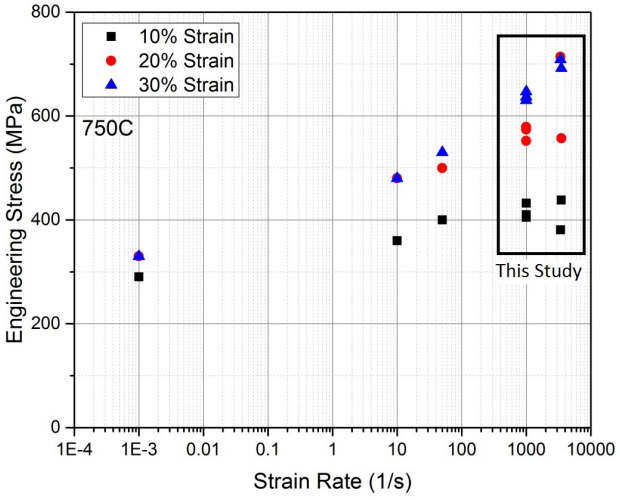

(*a*)

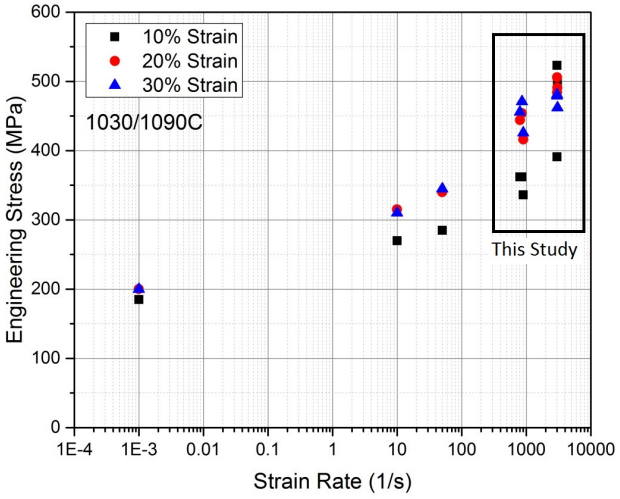

(*b*)

Fig. 10. Strain rate effect on the tensile stress-strain response at different temperatures (a) 750^oC and (b) 1030 or 1090^oC

5 Acknowledgements

The authors would like to acknowledge the support of Dr. Helena Jin for the preliminary DIC work and Kevin Connelly for his initial specimen and fixture design support.

This work was sponsored by the United States Department of Energy (DOE) Office of Space and Defense Power Systems (NE-75). The authors gratefully acknowledge the support and guidance of Ryan D. Bechtel of the US Department of Energy.

Sandia National Laboratories is a multi-program laboratory managed and operated by Sandia Corporation, a wholly owned subsidiary of Lockheed Martin Corporation, for the U.S. Department of Energy's National Nuclear Security Administration under contract DE-AC04-94AL85000.

Oak Ridge National Laboratory is a multi-program research laboratory managed by UT-Battelle, LLC, for the US DOE under contract DE-AC05-00OR22725.

References

1. Ohriner EK, Platinum Metals Review **52**, (2008) 186-197
2. George TG, *Los Alamos National Laboratory Report*, (1998) LA-11065
3. Schneibel JH, Carmichael CA, George, EP, *Oak Ridge National Laboratory Report*, (2007) ORNL/TM-2007/81
4. McKamey CG, George EP, Lee EH, Ohriner EK, Cohron JW, Scripta Material **42**, (2000) 9-15
5. George EP, Bei H, Lee EH, Braden JD, *Oak Ridge National Laboratory Report*, (2004) ORNL/TM-2004/239
6. Song B, Nelson K, Lipinski R, Bignell J, Ulrich G., George EP, Strain, (2014) DOI: 10.1111/str.12100 (in press)
7. Song B, Nelson K, Lipinski R, Bignell J, Ulrich G., George EP, *Sandia Report*, (2014) SAND2014-15442
8. Kolsky H, Proceeding of Royal Society of London **B62**, (1949) 676-700
9. Harding J, Wood EO, Campbell JD, Journal of Mechanical Engineering Science **2**, (1960) 88-96
10. Baker WE, Yew CH, Journal of Applied Mechanics **33**, (1966) 917-923
11. Chen W, Song B, *Split Hopkinson (Kolsky)Bar, Design, Testing and Applications*, (Springer, New York, 2011)
12. Kawata K, Hashimoto S, Kurokawa K, Kanayama N, in *Mechanical Properties at High Rates of Strain*, edited by J. Harding, **47**, (1979) 71-80
13. Owens, AT, Tippur HV, Experimental Mechanics **49**, (2009) 799-811
14. Song B, Antoun BR, Connelly K, Korellis J, Lu W-Y, Measurement Science and Technology **22**, (2011) 045704
15. Su J, Guo W, Meng W, Wang J, Mechanics of Materials **65**, (2013) 76-87
16. Guo W-G, Gao X, Materials Science and Engineering A **561**, (2013) 468-476
17. Feng, F, Huang S, Meng Z, Hu J, Lei Y, Zhou M, Wu D, Yang Z, Materials and Design **57**, (2014) 10-20
18. Whittington WR, Oppedal AL, Turnage S, Hammi Y, Rhee H, Allison PG, Crane CK, Horstemeyer MF, Materials Science and Engineering A **594**, (2014) 82-88
19. Vilamosa V, Clausen AH, Fagerholt E, Hopperstad OS, Bϕrvik T, Strain **50**, (2014) 223-235
20. Scapin M, Peroni L, Fichera C, Materials at High Temperatures **31**, (2014) 131-140
21. Song B, Lu W-Y, in *Proceedings of SEM XII International Congress and Exposition on Experimental and Applied Mechanics, Costa Mesa, CA 2012*